MINISTRY OF AVIATION

AERONAUTICAL RESEARCH COUNCIL

CURRENT PAPERS

A Wind Tunnel Investigation into the Pressure Distribution on a Wing Surface in a Non-Uniform Supersonic Flow

by

M. C. P. Firmin, M.Sc. and W. J. Bartlett, B.Sc., A.F.R.Ae.S.

LONDON: HER MAJESTY'S STATIONERY OFFICE

1961

PRICE 5s. 6d. NET

C.P. No.551

U.D.C. No. 533.69.048.2 : 533.693 : 533.6.011.5

February, 1960

A WIND TUNNEL INVESTIGATION INTO THE PRESSURE DISTRIBUTION ON A WING SURFACE IN A NON-UNIFORM SUPERSONIC FLOW

by

M. C. P. Firmin, M.Sc.
and
W. J. Bartlett, B.Sc., A.F.R.Ae.S.

SUMMARY

Using experimental and theoretical methods it is shown that linearized theory may be used to determine the pressure distribution on a wing surface in a non-uniform flow field caused by a streamwise line vortex.

It is demonstrated that a free vortex passing over a surface induces pressure and suction peaks on respective sides of the spanwise station of the vortex. These peaks are situated along Mach lines and are attenuated chordwise. It is found necessary to include the cross-flow terms in determining the theoretical pressure distribution.

Previously issued as R.A.E. Tech Note No. Aero 2673 - A.R.C.22,082.

LIST OF CONTENTS

LIST OF APPENDICES

LIST OF ILLUSTRATIONS

1 INTRODUCTION

In the prediction of longitudinal and lateral characteristics of an aircraft it is necessary to be able to estimate with fair accuracy the effect of a non-uniformity of the flow field on the aerodynamic forces acting on the aircraft surfaces. The case considered here is a supersonic stream containing crosswise velocity components such as are produced by free vortices.

Several approximate theoretical methods are available for the pressure distribution on a wing surface of moderate chord in a non-uniform stream. It is also known that the assumptions of linearised theory give adequate results for wings of moderate chord in a uniform stream but no satisfactory experimental evidence exists when the stream is non-uniform. The object of this investigation is, therefore, to find out whether it is adequate to treat the non-uniform velocity components as small perturbations of a uniform stream. This investigation covers effects on wings with supersonic leading edges; an investigation for wings with subsonic leading edges has not yet been undertaken.

The interference between the wing and an aft tailplane on conventional aircraft is a simple case when the tail surface is considerably smaller than the forward wing but still of high aspect ratio. It is then adequate to regard the tail as being located in a uniform downwash field, the effective incidence on the tailplane being taken as the mean incidence and obtained from the strength and position of the wing vortices. The interference load is then the product of the lift curve slope of the tail and the mean downwash. This method may not, however, be satisfactorily applied to aircraft where the surface affected has a large chord and where the downwash field is markedly non-uniform over the span of the wing surface[1,2] as is typical of canard configurations.

The work described here is an attempt to examine in some detail the pressure distribution induced on a wing by the non-uniform flow field downstream of a lifting foreplane; to develop a theoretical method of prediction, using linearised theory; and to formulate the condition when this is inadequate. The method should then be applicable to lifting surfaces in any other flow made non-uniform by the existence of downwash and sidewash velocities.

A second experimental programme, extending the range of investigation and relating the pressure distributions to overall forces and moments, is currently in progress.

2 THE ESTIMATION OF FOREPLANE-WING INTERFERENCE EFFECTS

2.1 Velocity components

In order to determine the pressure distribution on the rear wing surface due to a foreplane, it is necessary to know the flow in which the wing is immersed. Briefly, the physical picture is that the pressure distribution around any lifting wing causes an inward flow of air over one surface and an outward flow over the other. The resulting discontinuity in spanwise velocity at the trailing edge forms a vortex sheet which, as it passes downstream, rolls up into a pair of line vortices.

In this treatment it is assumed that the flow behind the foreplane (or generating surface) is fully rolled up at the rear wing location; then the flow field may be represented by that of a single rectangular horseshoe vortex[3]. The velocity components caused by an elementary line vortex in a supersonic flow as shown in Fig.1, with arms along OX_v, OY_v are given by:-

$$w_v = \frac{\Gamma}{2\pi} \cdot \frac{-X_v Y_v \left[\beta^2\left(Y_v^2 + 2Z_v^2\right) - X_v^2\right]}{\left(X_v^2 - \beta^2 Z_v^2\right)\left(Y_v^2 + Z_v^2\right)\sqrt{X_v^2 - \beta^2\left(Y_v^2 + Z_v^2\right)}} \qquad (1)$$

within the Mach cone from 0, $w_v = 0$ elsewhere.

$$v_v = \frac{\Gamma}{2\pi} \cdot \frac{X_v Z_v}{\left[Y_v^2 + Z_v^2\right]\sqrt{X_v^2 - \beta^2\left[Y_v^2 + Z_v^2\right]}} \qquad (2)$$

within the Mach cone from 0, $v_v = 0$ elsewhere.

It is evident that for points where $\beta^2 Z_v^2$ may be neglected compared with $X_v^2 - \beta^2 Y_v^2$ the velocity components within the Mach cone from 0 become:-

$$w_v = \frac{\Gamma}{2\pi} \frac{Y_v}{Y_v^2 + Z_v^2}\left\{1 - \frac{\beta^2 Y_v^2}{X_v^2}\right\}^{\frac{1}{2}} \qquad (3)$$

and

$$v_v = \frac{\Gamma}{2\pi} \frac{Z_v}{Y_v^2 + Z_v^2}\left\{1 - \frac{\beta^2 Y_v^2}{X_v^2}\right\}^{-\frac{1}{2}} \qquad (4)$$

2.2 Pressure distribution due to a line vortex

The flow from the foreplane immerses the rear wing in a non-uniform flow which produces a non-uniform pressure distribution on the wing surface. We can appreciate some of the characteristics of the pressure distribution by considering the velocity distribution from a line vortex, the downwash component of which is sketched on page 6.

The pressure distribution from a chordwise element of surface at incidence relative to its surroundings will give a concentration of pressure near the Mach lines from the leading edge. If elements of this form may be taken to represent the downwash shown then the pressure distribution on the wing surface will be of the form given in the sketch with the peak changes in pressure occurring along Mach lines from the leading edge.

There will also be a contribution to the pressure distribution due to the sidewash velocity which will take the form of a suction peak under the centre of the vortex.

We may derive an analytical expression for the pressure distribution on the wing surface within the limitations of linearised theory. These assumptions of linearised theory are as follows.

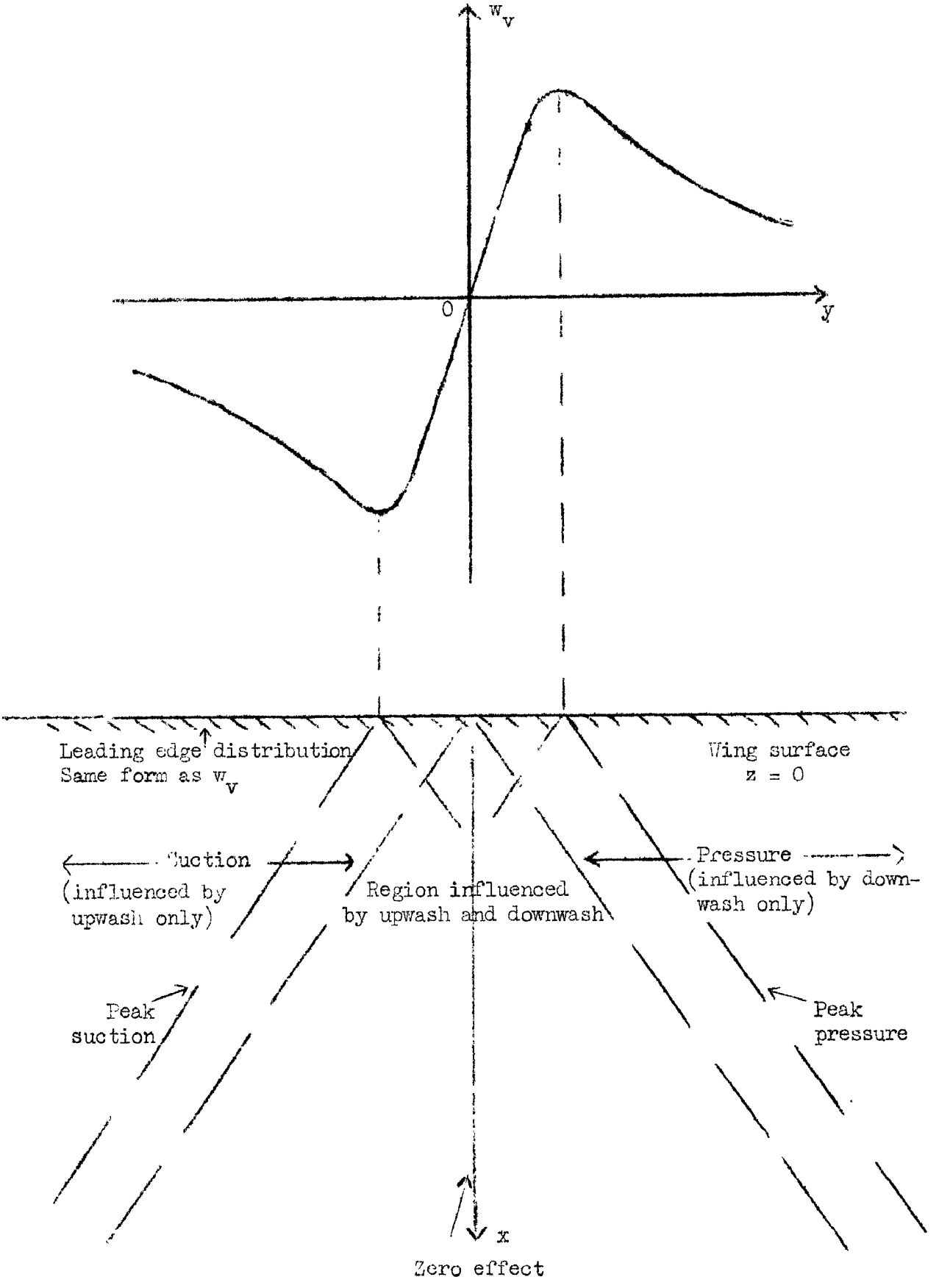
w_v
0
y
Leading edge distribution
Same form as w_v
Wing surface
z = 0
Suction
(influenced by
upwash only)
Region influenced
by upwash and downwash
Pressure
(influenced by down-
wash only)
Peak
suction
Peak
pressure
x
Zero effect

1 The viscosity of the air is neglected.

2 The heat conductivity of the air is neglected.

3 The flow field is free of vorticity (and thus possesses a velocity potential) except for certain singular points.

4 All external force fields are excluded.

5 The equation of state for a perfect gas holds.

6 The perturbation velocities are small compared with the free stream velocity.

Since supersonic aerofoil theory, based on these same assumptions, is known to give adequate results for wings in a uniform stream, it is really the first and last assumptions which are questioned in the present context. The object of this investigation is, therefore, to find out whether it is adequate to treat the non-uniform velocity components as small perturbations of the stream and, further, whether the simple model of an inviscid line vortex, as has been supposed in para. 2.1, is sufficient to represent the actual rolled-up vortex sheet with viscous core.

Within the above limitations we may consider the flow as a linear combination of two flows:-

(a) The flow due to the generating surface (line vortex) alone.

(b) A twisted and cambered wing in a uniform stream with the boundary condition $w = -w_v$ at $z = 0$.

The boundary condition for the combined flow then gives $w = 0$ at the wing surface.

It is well known[4] that, within the limits of the linearised theory, we may replace a wing surface in a uniform stream by a source distribution. The local strength of the source distribution is determined by the downwash perturbation velocity at all points within the forward Mach cone from P (see Fig.1).

The velocity potential due to a source distribution is:-

$$\varphi(x,y,z) = -\frac{1}{\pi}\int\int_A \frac{w_{z=0}\, d\xi\, d\eta}{\sqrt{(x-\xi)^2 - \beta^2[(y-\eta)^2 + z^2]}} , \qquad (5)$$

where A is the area of the wing within the forward Mach cone from P.

We are limited to supersonic leading edges since w is given only on the wing area. This method has, however, been extended[5] to give solutions at the wing surface ($z = 0$) in a tip region by modifying the area of integration.

This source method makes it theoretically possible to find the perturbation velocities at P due to the presence of the wing. It has not been found possible to obtain a solution in closed form for the general downwash distribution given in equation (1) but solutions have been obtained for certain approximations to this distribution.

The first approximation is to take X_v^2 large compared with Y_v^2 in equation (3) which gives

$$w_v = \frac{\Gamma}{2\pi} \frac{Y_v}{Y_v^2 + Z_v^2} \quad ; \tag{6}$$

this is the downwash velocity from an infinitely long line vortex.

The pressure distribution associated with this downwash distribution is derived in Appendix 1 and given by:-

$$C_p = - \frac{\Gamma \, \text{sign}(A) \sqrt{\{(A^2 - B^2 - 1)^2 + 4A^2\}^{\frac{1}{2}} + A^2 - B^2 - 1}}{\sqrt{2}\, \pi U Z_v \beta \sqrt{(A^2 - B^2 - 1)^2 + 4A^2}} \tag{7}$$

where $A = \frac{y}{Z_v}$, and $B = \frac{x}{Z_v \beta}$.

The form of this distribution of pressure is shown in Fig. 3 and exhibits the main features discussed previously (i.e. suction and pressure peaks on Mach lines) together with a region between the peaks where the velocity distribution chosen has little effect. Another feature of this distribution is the attenuation of the suction and pressure peaks with distance from the leading edge.

Integration of the load distribution obtained from the above pressure distribution for a pair of vortices over a region of infinite chord and large span but not influenced by 'tip' regions gives a load equal and opposite to that acting on the surface which produces the vortices.

It is possible to obtain an approximation to the effect of finite X_v on the pressure distribution by taking a second approximation to the downwash velocity given in equation (3). Then

$$w_v = \frac{\Gamma}{2\pi} \frac{Y_v}{Y_v^2 + Z_v^2} \left(1 - \frac{\beta^2 Y_v^2}{2 X_v^2}\right) . \tag{8}$$

The effect of taking this approximation for w_v has been found in Appendix 2 to be:-

$$\Delta C_p = \frac{C_p |A| \sqrt{(A^2 - B^2 - 1)^2 + 4A^2}}{\sqrt{2} \left(\frac{B}{2} + C\right)^2 \sqrt{[(A^2 - B^2 - 1)^2 + 4A^2]^{\frac{1}{2}} + A^2 - B^2 - 1}} \tag{9}$$

where $C = \frac{d}{\beta Z_v}$. This is proportional to the spanwise location and varies as the inverse square of the distance between the generating surface and the chordwise location of the point on the wing.

Further approximations may be made by the method adopted in Appendix 2.

When a free vortex passes near to a surface, the cross flow velocities, which have so far been ignored, are not generally small enough for the approximations of linearised theory to be confidently applied, and the effect of the cross flow must be considered.

The cross flow velocity induced by the surface due to an infinite straight vortex has been determined by the source distribution method in Appendix 3, where it is shown that for large distances from the leading edge the induced cross flow velocity is the same as that obtained by the exact method of images.

The pressure distribution can now be obtained from the second order approximation to Bernoulli's equation

$$C_P = -\frac{2}{U}\frac{\partial\varphi}{\partial x} + \frac{\beta^2}{U^2}\left(\frac{\partial\varphi}{\partial x}\right)^2 - \frac{1}{U^2}\left(\frac{\partial\varphi}{\partial y} + v_v\right)^2 - \frac{1}{U^2}\left(\frac{\partial\varphi}{\partial z} + w_v\right)^2 . \qquad (10)$$

At the wing surface we have $\frac{\partial\varphi}{\partial z} = -w_v$; if $\frac{\beta^2}{U^2}\left(\frac{\partial\varphi}{\partial x}\right)^2$ may be neglected, then

$$C_P \doteq -\frac{2}{U}\left(\frac{\partial\varphi}{\partial x}\right) - \frac{1}{U^2}\left(\frac{\partial\varphi}{\partial y} + v_v\right)^2 . \qquad (11)$$

It should be noted that there is a contribution to the loading from from this extra term due to the cross product $\frac{2v}{U^2}\frac{\partial\varphi}{\partial y}$, since $\frac{\partial\varphi}{\partial y}$ is discontinuous across $z = 0$.

The above solution has been obtained for a straight vortex which is only valid for $\frac{x}{\beta Z_v}\left(\frac{x}{\beta Z_v} - 2\right) < \frac{y^2}{Z_v^2}$, $Z_v > 0$ and all $\left(\frac{x}{\beta Z_v}, \frac{y}{Z_v}\right)$ for $Z_v < 0$.

Outside this region the vortex will be influenced by the flow field induced by the wing surface and will curve along a path determined by the streamlines. If the vortex is assumed straight, it will sustain a force which makes the solution unacceptable outside the region indicated.

Modification of the pressure equation as described above gives a suction peak under the vortex which is quite large when the vortex is close to the surface (see section 4).

For large distances from the leading edge the wing may be considered as a reflection plate and the flow due to the free vortex will induce flow equivalent to an image vortex below the surface.

The pressure distribution due to such a system has been determined in Appendix 4 to be

$$C_P = \frac{\Gamma^2}{2\pi^2 U^2 Z_v^2}\,\frac{(A+D)^2 - 1}{\{(A+D)^2 + 1\}^2} , \qquad (12)$$

where $D = \frac{\Delta S_o'}{Z_v}$. The load from such a spanwise distribution is zero, if taken over a large span.

2.3 Circulation

In determining the actual magnitude of the pressure coefficient the location and strength of the foreplane vortices are required.

These may be determined from linearized theory since the lift associated with a vortex pair ($L = \Gamma \rho U 2 S_o'$) is equal to that generated on the foreplane; neglecting any viscous dissipation we have:-

$$\frac{\Gamma}{U} = \frac{1}{2}\int_0^{c_o} \Delta C_p \, dx = \frac{\pi}{90} \frac{c_o \delta}{\beta} \qquad (13)$$

and

$$S_o' = S_o \left(1 - \frac{1}{2A' \beta}\right) . \qquad (14)$$

3 DESCRIPTION OF THE WIND TUNNEL TESTS

Wind tunnel tests have been made to examine experimentally the pressure distribution induced on a wing by the flow field from a lifting foreplane. The experimental pressure distribution may then be compared with the theoretical methods of prediction using linearised theory and the conditions when this is inadequate may be formulated.

Fig.2 shows the main details of the model which was fixed to the side-wall of the tunnel and the reflection-plate technique used. The forward generating surface could be set to a required incidence and the height of its hinge line relative to the rear wing surface altered by using different mounting holes. In this way it was possible to alter the non-uniform flow field at the rear surface.

The rear surface was set at zero incidence to the main stream. Static pressure holes in the surface were connected to a water manometer, the reference pressure being the static pressure within the tunnel working section. The pressure distribution due to the forward surface was then found by obtaining the difference between the results with and without the generating surface present.

Two series of tests were made in the R.A.E. No.18, (9" × 9") supersonic wind tunnel at a Mach number of 1.81 under atmospheric stagnation conditions. The first gave the general distribution of pressure over the whole surface, the resolution being limited by the number of pressure plotting tubes that could be taken through the support of the model. The second set was restricted to obtaining in more detail the pressure distribution at one chordwise position.

During the above tests the location of the vortex generated by the fore-plane was obtained at various streamwise positions using a pitot tube to locate the position of minimum pressure, which has been taken to be the centre of the vortex since the measured pressures were symmetrical about this point.

The circulation of the vortex has also been determined experimentally using a yawmeter. The yawmeter consisted of four one-millimetre hypodermic tubes symmetrically enclosed in a length of three-millimetre tubing, the head being ground down to a four-sided 90° pyramid with one tube in the middle of each face. Thus, simultaneous measurements of upwash and sidewash angles were made by observing the pressure difference registered by the vertical and horizontal pairs of holes respectively.

The circulation within a contour is defined by the line integral

$$\Gamma = \int_C \underline{q} \cdot \underline{dS} , \qquad (15)$$

and if we take the contour C to be a rectangle A B C D, then

$$\Gamma = \int_A^B v' \, dy + \int_B^C w' \, dz - \int_C^D v' \, dy - \int_D^A w' \, dz ;$$

therefore:-

$$\frac{\Gamma}{U} = \left\{ \int_A^B - \int_C^D \right\} \beta' \, dy + \left\{ \int_B^C - \int_D^A \right\} \alpha' \, dz ,$$

where α', β' are the upwash and sidewash angles measured with the yawmeter.

Each of the above integrals was evaluated graphically and thus the circulation determined.

When using the above method, care must be taken to choose a contour such that the integrated effect of pressure gradients across the yawmeter cancel out.

4 DISCUSSION OF THE EXPERIMENTAL RESULTS

4.1 Surface pressure measurements

The experimental pressure differences obtained on the rear surface have been presented in terms of the coefficient of pressure developed due to the generating surface. The location of the pressure holes is given in non-dimensional form and related to the measured location of the vortex at the leading edge of the rear wing surface.

Fig.4 shows the experimental surface pressure measurements obtained for a vortex passing at 0.41 foreplane chords above the wing surface with a circulation given by $\frac{\Gamma}{U c_o} = 0.21$. This pressure distribution has pressure and suction peaks on Mach lines from the leading edge and shows qualitative agreement with the linearised theory distribution given in Fig.3. There is also a suction peak under the centre of the vortex which was anticipated as the effect of the cross-flow.

In the region $\frac{x}{\beta Z_v} - \frac{y}{Z_v} > 7.0$ the image of the vortex in the reflection plate is likely to affect the flow; this may account for the increase in pressure observed in this region.

A more detailed comparison between the experimental and theoretical pressure distribution is given in Fig.5, for the station nearest to the leading edge. In this figure a first approximation to the effect of the finite distance between the foreplane and rear surface is given as described in

para 2.2; this is only strictly applicable to regions A (Fig.1) where $\eta^2 << \beta^2 X_v^2$. It is, however, an underestimation of the effect, since the approximation for w falls off more slowly with spanwise distance from the vortex than in equation (4).

Fig.6 gives the pressure distribution for the same station with the vortex much closer to the wing surface. Due to the relatively sudden changes in pressure the experimental readings are not sufficient to define an experimental curve over the complete range. The points do, however, indicate that some suction occurs under the vortex.

The results of a second set of tests are, however, more conclusive. Figs.7 and 8 give the pressure distribution, at about the mid chord position, for the same setting as Figs.5 and 6 respectively. Fig.7 illustrates the need to incorporate the cross-flow terms when calculating a pressure distribution.

Fig.8 gives the pressure distribution when the vortex is near the surface for a comparatively large $\frac{x}{\beta Z_v}$. The sidewash velocities at points on the surface nearest to the core have theoretically reached sonic speed, and therefore one would not expect linearised theory to predict accurately the pressure distribution. It is, however, found that the experimental pressure distribution still has the form predicted by linearised theory at points away from the vortex core, but the peaks have been rounded off due, presumably, to viscous effects predominating where large pressure gradients exist. The finite extent of the vortex core must also have an appreciable effect in this case. At points on the surface nearest to the vortex core the inclusion of cross-flow terms due to a straight vortex is not acceptable in the region indicated, since as mentioned in para. 2.2, the vortex would sustain a force if held straight as has been assumed. At a large distance from the leading edge $\left(\text{i.e. large } \frac{x}{\beta Z_v}\right)$ the wing surface may be considered as a reflection plate and the flow due to the free vortex will induce flow equivalent to an image vortex below the surface. The effect of using the cross-flow velocities for such a system is also shown. Viscous effects may be expected to influence the pressure distribution in this region due to the large pressure gradients predicted by the theoretical method. This probably accounts for the relatively small changes in pressure found under the core of the vortex.

4.2 Vortex path

Measurements of the location of the core of the vortex at various streamwise positions have been made using a pitot tube. The results for several settings of the generating surface are given in Fig.9. It will be noted that the movements of the core of the vortex are comparatively small and depend on the directions of the cross-flow induced by the presence of the wing surface. Since the induced flow depends on the direction of the circulation so also does the movement of the vortex core. In Fig.10 a comparison has been made between the core path found experimentally and that given theoretically assuming the linear theory sidewash velocities and the vortex remains along a streamline from all other sources except the vortex itself.

The main features to be noted are that, when the core is close to the surface of the wing, the vortex appears to have been disturbed upstream of the wing leading edge, indicating that the effect of the wing is transmitted upstream either by local detached shockwaves or in the core of the vortex. There is fair agreement between the changes in span indicated by the theory and those found experimentally for $1 < \frac{x}{Z_v \beta} < 3$. Further aft the vortex

tends to return towards the main stream direction, and does not approach the asymptotic solution, indicating possibly a reduction in sidewash velocities in this region, or some kind of transmission in the core of the vortex as suspected upstream of the wing leading edge. The minimum slope expected at large distances from the wing leading edge using the asymptotic solution is also given.

4.3 Circulation of vortex

The circulation of the vortex shed from the generating surface has been found at three longitudinal locations by measuring the direction of the flow at points round a contour with a yawmeter as described in section 3.

It was found that the value obtained for the circulation was not appreciably affected by the size of the contour traversed provided the path was chosen so that the integrated effect of pressure gradients across the yawmeter cancelled out. For example, a contour with one side passing within about 0.8 yawmeter head diameters of the vortex core gave a result within 1.5% of that obtained when this distance was increased to 2.5 diameters.

The results of the measurements taken are given in the table below. The measurements show the experimental value to be about 6% lower than the result obtained from simple linear theory considerations. There is also a consistent drop of about 5% between the results fore and aft of the wing leading edge disturbance, which is not yet understood since the drop does not, apparently, depend on the distance of the vortex from the surface of the wing or the distance aft of the wing leading edge disturbance. It was not possible to traverse round the vortex when it was close to the surface of the wing due to the size of the yawmeter used; therefore it was impossible to check the cause of the drop in sidewash velocity predicted by the locus of the vortex given in Fig.10(a). The results found here are not inconsistent with a redistribution in circulation suggested by the locus of the vortex cores, or some unrolling of the vortex. It will, however, be necessary to make further tests before any definite conclusion can be reached.

δ Degrees	h Inches	$\frac{x}{\beta Z_v}$	$\frac{\Gamma}{U c_o}$ (Exp)	$\frac{\Gamma}{U c_o}$ (Theory)
9.9	0.25	Ahead of wing	0.208	0.220
10.1	0.50	Ahead of wing	0.212	0.225
9.9	0.25	2.8	0.200	
10.1	0.50	1.5	0.201	
10.1	0.50	2.7	0.201	

5 OUTSTANDING PROBLEMS AND WORK IN PROGRESS

5.1 Pressure distribution

The work described in this report has dealt as fully as present methods allow with the pressure distribution due to a vortex passing over a surface with a non-swept leading edge.

One problem that requires consideration is the effect of a free vortex on a surface with a swept leading edge.

The pressure distribution may be obtained theoretically by the source distribution method for supersonic leading edges and a modified source distribution method for subsonic edges, provided edge separations do not occur[6,7].

The load acting on a delta wing with supersonic leading edges, due to a pair of free vortices passing over one surface, may become infinite if calculated by the source distribution method (neglecting cross-flow), for wings of very large area. This result is physically unrealistic. The slender body result for highly swept wings[8,9] gives a much more realistic result in that the maximum load is independent of the wing area and leading edge shape and depends only on the load generating the non-uniform flow. These results need further investigation.

It is proposed to make a series of tests to determine in more detail the pressure distribution over a rectangular wing surface - including the 'tip' regions. The wing will be mounted from the rear on a traversing gear thus enabling all relative locations with respect to the foreplane to be tested. The foreplane will be further ahead of the rear wing surface than in the present tests but it will be possible to alter the fore and aft location of the rear wing enabling the effect of the Mach cones from the foreplane to be investigated.

From this new set of tests it is also hoped to be able to integrate the pressure distribution with enough accuracy to determine the load changes with increase in chord and also to determine the rolling moment due to sideslip.

The pressure distribution in the 'tip' region due to a free vortex passing near it will test the validity of the modified source distribution method, which is applicable to both 'tip' regions and slender wings, near the 'tips' where separations are likely to occur. This work may lead to a method of calculating the pressure distribution on a slender wing in the presence of free vortices and leading edge separations.

A series of tests on a delta wing with supersonic leading edges is also planned, to establish the validity of the source distribution both in the region not influenced by the apex (i.e. two-dimensional yawed wing region) and in the region affected by the apex of the wing.

In general, it is clear that a better knowledge of the detailed structure of the vortex is required if a closer representation of the actual pressures than that obtained with the simple line vortex is wanted.

5.2 Force measurements

Because of the nature of the pressure distribution due to the foreplane vortices, and the limitation in the number of pressure points, the lift and moments developed on rear wing surfaces will, if found from pressure measurements, be of poor accuracy. It is therefore proposed to make another series of tests to measure the lift, pitching moment and rolling moment developed on a series of rectangular and slender delta wings of various aspect ratios. These tests should enable a check to be made on existing theoretical methods[8,9,10,11] for the forces developed due to the foreplane vortices, and also produce some fundamental results on rolling moment due to sideslip.

It is also the aim of this work to obtain an empirical law connecting the maximum load ratio (i.e. maximum interference load as a fraction of foreplane load) as a function of span ratio (i.e. ratio of span of rear surface at trailing edge to that of the Mach envelope from the foreplane). This should enable an empirical correction factor to be obtained for the finite distance between foreplane and rear surface.

6 CONCLUSIONS

It has been shown that the pressure distribution on a wing surface due to a free vortex has pressure and suction peaks on Mach lines from the points of maximum local incidence at the leading edge and these are attenuated in a chordwise direction. A theory based on the assumption of small perturbations and on the simple model of an inviscid line vortex gives adequate results in most cases.

At points on the surface near the core of the vortex a correction to the theoretical calculations is necessary due to the cross-flow and it is suggested that the sidewash velocity given by the linear theory is a good approximation in regions not influenced by the bending of the vortex.

When the vortices pass very close to the rear surface and the cross-flow velocities are theoretically approaching sonic speed large pressure gradients theoretically occur and the approximations of linearised non-viscous theory fail to show other than the form of the pressure distribution since the effects of the cross-flow compressibility and viscosity are neglected. The detailed structure of the rolled-up sheet and its viscous core should then also be taken into account.

The vortices are disturbed by the rear wing surface and the results suggest that a vortex does not change strength up to a few vortex core diameters of the surface, when the sidewash velocities suggest either some redistribution of circulation or unrolling of the vortex core.

LIST OF SYMBOLS

OX_v, Y_v, Z_v	right hand system of axes fixed relative to a rectangular vortex element
Ox,y,z	right hand system of axes fixed in rear wing surface (Fig.1)
A'	aspect ratio of foreplane
c_o	chord of foreplane
C_P	wing upper surface pressure coefficient $= \dfrac{P - P_s}{\frac{1}{2}\rho U^2}$
h	height of foreplane relative to rear surface
d	distance between centre line of foreplane and leading edge of rear surface
L	lift generated on foreplane
M	Mach number
P	wing surface static pressure
P_s	static pressure in undisturbed stream
S_o	semi-span of foreplane

LIST OF SYMBOLS (Contd.)

S_o'	semi-span of vortex pair
$\Delta S_o'$	change in semi-span of vortex pair aft of leading edge of rear surface
U	free stream velocity
v_v	sidewash velocity due to a rectangular vortex element
w_v	downwash velocity due to a rectangular vortex element
v'	measured sidewash velocity
w'	measured downwash velocity
α'	$\frac{w'}{U}$, downwash angle measured by yawmeter
β'	$\frac{v'}{U}$, sidewash angle measured by yawmeter
β	$\sqrt{M^2 - 1}$
Γ	circulation of vortex
δ	foreplane incidence setting - degrees
ξ, η	co-ordinates of an elemental source in Ox,y plane
ρ	density
φ	perturbation velocity potential due to wing

LIST OF REFERENCES

No.	Author(s)	Title, etc.
1	Watts, P.E. Beecham, L.J.	A wind tunnel investigation of the longitudinal and lateral aerodynamic characteristics of a canard aircraft model. Part 1 - Tests at M = 1.40 and M = 2.02. A.R.C. R & M 3226. February, 1959.

LIST OF REFERENCES (Contd.)

No.	Author(s)	Title, etc
2	Watts, P.E. Treadgold, D.A.	A wind tunnel investigation of the longitudinal and lateral aerodynamic characteristics of a canard aircraft model. Part II - Tests at M = 2.47. A.R.C. R & M 3226. February, 1959.
3	Mirels, H. Haefeli, R.C.	Line vortex theory for the calculation of supersonic downwash. N.A.C.A. Tech. Note No. 1925. August, 1949.
4	Puckett, A.E.	Supersonic wave drag of thin airfoils. J. Ae. Sci. September, 1946.
5	Evvard, J.C.	Theoretical distribution of lift on thin wings at supersonic speeds (an extension). N.A.C.A. Tech. Note 1585. May, 1948.
6	Etkin, B. Woodward, F.	Lift distribution on supersonic wings with subsonic leading edges and arbitrary angles of attack. Proceedings of second Canadian symposium on aerodynamics. Inst. of Aerophysics. 1954.
7	Etkin, B.	Numerical integration methods for supersonic wings in steady and oscillatory motion. U.T.1A Report No.36. November, 1955.
8	Sacks, A.H.	Aerodynamic interference of slender wing-tail combinations. N.A.C.A. Tech. Note 3725. January, 1957.
9	Sacks, A.H.	Vortex interference effects on the aerodynamics of slender airplanes and missiles. J. Ae. Sci. June, 1957.
10	Owen, P.R. Maskell, E.C.	Interference between the wings and the tailplane of the slender wing-body-tail combination. A.R.C. 14,483. October, 1951.

LIST OF REFERENCES (Contd.)

No.	Author(s)	Title, etc
11	Alden, H.L. Schindel, L.H.	The lift, rolling moment and pitching moment on wings in nonuniform supersonic flow. J. Ae. Sci. January, 1952.
12	Bolton-Shaw, B.W.	The lifting pressure distribution on a finite wing with supersonic leading edge, with wing twist or stream incidence or both varying arbitrarily in a spanwise direction. English Electric Co. Ltd. Report No. L.A.T.033. June, 1952.

APPENDIX 1

THE ESTIMATION OF THE LINEAR THEORY PRESSURE DISTRIBUTION ON A WING SURFACE DUE TO AN INFINITE STRAIGHT VORTEX

If we follow the source distribution given by Puckett[4] for the velocity potential at a point P(x,y,z) in linearised flow we have

$$\varphi(x,y,z) = -\frac{1}{\pi}\int_A \frac{w\, d\xi\, d\eta}{\sqrt{(x-\xi)^2 - \beta^2[(y-\eta)^2 + Z^2]}} \tag{16}$$

and from this using the results of Bolton-Shaw[12] we may obtain

$$C_P = -\frac{2}{U}\left(\frac{\partial\varphi}{\partial x}\right)_{Z=0} = \frac{2}{\pi\beta}\int_0^\pi f(y + \frac{x}{\beta}\cos\theta)d\theta \tag{17}$$

where $\frac{w}{U} = f(\eta)$, provided the downwash velocity at the wing plane is independent of ξ.

If we take

$$\frac{w}{U} = \frac{-\Gamma}{2\pi U}\,\frac{\eta}{(\eta^2 + Z_v^2)} \tag{18}$$

i.e. a vortex parallel to the x axis at a height Z_v above the z = 0 plane, then we have

$$C_P = \frac{-\Gamma}{\pi^2 U \beta}\int_0^\pi \frac{\left(y + \frac{x}{\beta}\cos\theta\right)d\theta}{\left(y + \frac{x}{\beta}\cos\theta\right)^2 + Z_v^2} \tag{19}$$

this may be split up into complex partial fractions and then integrated by contour integration, i.e.

$$C_P = \frac{-\Gamma}{\pi^2 U \beta}\, R\ell\left[\int_0^\pi \frac{d\theta}{y + \frac{x}{\beta}\cos\theta - i\, Z_v}\right]. \tag{20}$$

Let us now put $t = \tan\frac{\theta}{2}$ then

$$C_P = \frac{-2\Gamma}{\pi^2 U \beta}\, R\ell\left[\int_0^\infty \frac{dt}{\left(y + \frac{x}{\beta} - i\, Z_v\right) + \left(y - \frac{x}{\beta} - i\, Z_v\right)t^2}\right] \tag{21}$$

This suggests a contour integral, the contour consisting of the real axis (-R to +R) and a semi-circle of radius R with the origin as centre. This gives as $R \to \infty$

$$\int_0^\infty \frac{dt}{\left(y + \frac{x}{\beta} - i\,Z_v\right) + \left(y - \frac{x}{\beta} - i\,Z_v\right) t^2} = \frac{+\pi\, i\, \text{sign}\left(\frac{x}{\beta}\, Z_v\right)}{2\sqrt{-\left(y + \frac{x}{\beta} - i\,Z_v\right)\left(y - \frac{x}{\beta} - i\,Z_v\right)}}$$

$$(Z_v \neq 0) \quad \ldots\ldots (22)$$

Hence

$$C_P = \frac{-\Gamma\, \text{sign}\left(\frac{x}{\beta}\, Z_v\right)}{\pi U \beta}\, R\ell\left[\frac{i}{\sqrt{-\left(y + \frac{x}{\beta} - i Z_v\right)\left(y - \frac{x}{\beta} - i Z_v\right)}}\right] \qquad (23)$$

$$= \frac{-\Gamma\, \text{sign}\left(\frac{x}{\beta}\, Z_v\right) \cdot R\ell\left[i \sqrt{\frac{x^2}{\beta^2} - y^2 + Z_v^2 - 2i\, Z_v\, y}\right]}{\pi U \beta \sqrt{\left\{\left(y + \frac{x}{\beta}\right)^2 + Z_v^2\right\}\left\{\left(y - \frac{x}{\beta}\right)^2 + Z_v^2\right\}}} \qquad (24)$$

$$= \frac{-\Gamma\, \text{sign}\left(y\, \frac{x}{\beta}\right) \sqrt{\left[\left(\frac{x^2}{\beta^2} - y^2 + Z_v^2\right)^2 + 4\, Z_v^2\, y^2\right]^{\frac{1}{2}} - \frac{x^2}{\beta^2} + y^2 - Z_v^2}}{\sqrt{2}\, \pi\, U\, \beta \sqrt{\left(y^2 - \frac{x^2}{\beta^2} - Z_v^2\right)^2 + 4\, y^2\, Z_v^2}} \qquad (25)$$

which becomes in non-dimensional form

$$C_P = \frac{-\Gamma\, \text{sign}\,(A) \sqrt{\left[(A^2 - B^2 - 1)^2 + 4\, A^2\right]^{\frac{1}{2}} + A^2 - B^2 - 1}}{\sqrt{2}\, \pi\, U\, \beta\, Z_v \sqrt{(A^2 - B^2 - 1)^2 + 4\, A^2}} \qquad (26)$$

where $A = \frac{y}{Z_v}$ and $B = \frac{x}{Z_v\, \beta}$.

APPENDIX 2

AN APPROXIMATE CORRECTION FOR THE FINITE DISTANCE BETWEEN THE FOREPLANE AND WING SURFACE

If we follow the same method as Appendix 1 but take

$$\frac{w}{U} = \frac{-\Gamma}{2\pi U} \frac{\eta}{\eta^2 + Z_v^2} \left[1 - \frac{\beta^2 \eta^2}{2\left(d + \frac{x}{2}\right)^2} \right] \qquad (27)$$

instead of equation (18), where d is the distance between the foreplane and the wing leading edge.

This gives

$$C_P = \frac{-\Gamma}{\pi^2 U \beta} \int_0^{\pi} \frac{\left(y + \frac{x}{\beta} \cos\theta\right) d\theta}{\left(y + \frac{x}{\beta} \cos\theta\right)^2 + Z_v^2} + \frac{\Gamma \beta Z_v^2}{2\pi^2 U \left(d + \frac{x}{2}\right)^2} \int_0^{\pi} \left(y + \frac{x}{\beta} \cos\theta\right) d\theta \qquad \ldots\ldots (28)$$

on neglecting Z_v^2 compared with d^2,

$$\therefore \quad C_P = C_{P_I} + \frac{\Gamma \beta Z_v^2 y}{2\pi U \left(d + \frac{x}{2}\right)^2} \qquad (29)$$

where C_{P_I} is the pressure coefficient given in Appendix 1.

This gives

$$\frac{C_P - C_{P_I}}{C_{P_I}} = \frac{-|A| \sqrt{(A^2 - B^2 - 1)^2 + 4A^2}}{\sqrt{2}\left(\frac{B}{2} + C\right)^2 \sqrt{\left[(A^2 - B^2 - 1)^2 + 4A^2\right]^{\frac{1}{2}} + A^2 - B^2 - 1}} \qquad (30)$$

where $A = \frac{y}{Z_v}$, $B = \frac{x}{\beta Z_v}$ and $C = \frac{d}{\beta Z_v}$.

APPENDIX 3

THE ESTIMATION OF THE SIDEWASH VELOCITY PRODUCED BY A WING IN A FIELD DUE TO AN INFINITE STRAIGHT VORTEX BY A LINEAR THEORY METHOD

Following the same method as Appendix 1 we obtain

$$\frac{\partial \varphi}{\partial y} = \frac{U x}{\pi \beta^2} \int_{\eta_1}^{\eta_2} \frac{f(\eta)(\eta - y)d\eta}{\{(y-\eta)^2 + z^2\}\sqrt{x^2 - \beta^2[(y-\eta)^2 + z^2]}} \qquad (31)$$

which may be transformed to:-

$$\frac{\partial \varphi}{\partial y} = \frac{U x a}{\pi \beta^2} \int_0^{\pi} \frac{f(y + a\cos\theta)\cos\theta\, d\theta}{[a^2\cos^2\theta + z^2]} \qquad (32)$$

where $a = \sqrt{\left(\frac{x}{\beta}\right)^2 - z^2}$ but

$$f(\eta) = f(y + a\cos\theta) = \frac{\Gamma(y + a\cos\theta)}{2\pi U\{(y + a\cos\theta)^2 + Z_v^2\}}$$

$$\therefore \frac{1}{U}\frac{\partial \varphi}{\partial y} = \frac{\Gamma x a}{2 U \pi^2 \beta^2} \int_0^{\pi} \frac{(y + a\cos\theta)\cos\theta\, d\theta}{[a^2\cos^2\theta + z^2][(y + a\cos\theta)^2 + Z_v^2]} \qquad (33)$$

which may be split into complex partial fractions

$$\therefore \frac{1}{U}\frac{\partial \varphi}{\partial y} = \frac{\Gamma}{2\pi^2 U}\left[\int_0^{\pi} \frac{A\, d\theta}{+a\cos\theta - i z} + \int_0^{\pi} \frac{B\, d\theta}{+a\cos\theta + i z}\right.$$

$$\left. + \int_0^{\pi} \frac{C\, d\theta}{(y + a\cos\theta + i Z_v)} + \int_0^{\pi} \frac{D\, d\theta}{(y + a\cos\theta - i Z_v)}\right]$$

..... (34)

where

$$A = \frac{+\frac{x}{\beta}(y+iz)}{2[(y+iz)^2+Z_v^2]}, \qquad B = \bar{A}$$

and

$$C = \frac{-\frac{x}{\beta}(y+iZ_v)}{2[(y+iZ_v)^2+z^2]}, \qquad D = \bar{C}.$$

The integrals involved in equation (30) are the same form as in Appendix 1 (equation (20)).

Hence on collecting terms and simplifying we obtain:-

$$\frac{1}{U}\frac{\partial\varphi}{\partial y} = \frac{\Gamma}{2\pi U}\left[\frac{z(y^2+z^2-Z_v^2)}{(y^2+Z_v^2-z^2)^2+4y^2z^2}+\frac{x}{\sqrt{2}\beta}\left\{\frac{|Z_v|(y^2+Z_v^2-z^2)\sqrt{\lambda+\mu}}{\lambda([y^2+z^2-Z_v^2]^2+4y^2Z_v^2)}\right.\right.$$

$$\left.\left.-\frac{|y|(y^2+Z_v^2+z^2)\sqrt{\lambda-\mu}}{\lambda([y^2+z^2-Z_v^2]^2+4y^2Z_v^2)}\right\}\right]. \qquad (35)$$

where $\lambda^2 = \left(\frac{x^2}{\beta^2}-y^2-z^2+Z_v^2\right)^2+4y^2Z_v^2$

$$\mu = \frac{x^2}{\beta^2}-y^2-z^2+Z_v^2 .$$

Now when $x \to \infty$

$$\frac{1}{U}\frac{\partial\varphi}{\partial y} \to \frac{\Gamma}{2\pi U}\frac{(Z_v+z)}{y^2+(Z_v+z)^2} \qquad (36)$$

which is the sidewash velocity due to an infinite straight vortex situated at the image position with respect to the generating vortex.

APPENDIX 4

AN ESTIMATION OF THE PRESSURE DISTRIBUTION PRODUCED BY A FREE VORTEX PASSING OVER AN INFINITE PLANE

If we pass a line vortex in a uniform stream over an infinite plane then the plane must act as a reflection plate for the surface boundary conditions to be satisfied.

We will consider the case when the vortex will pass along a free streamline.

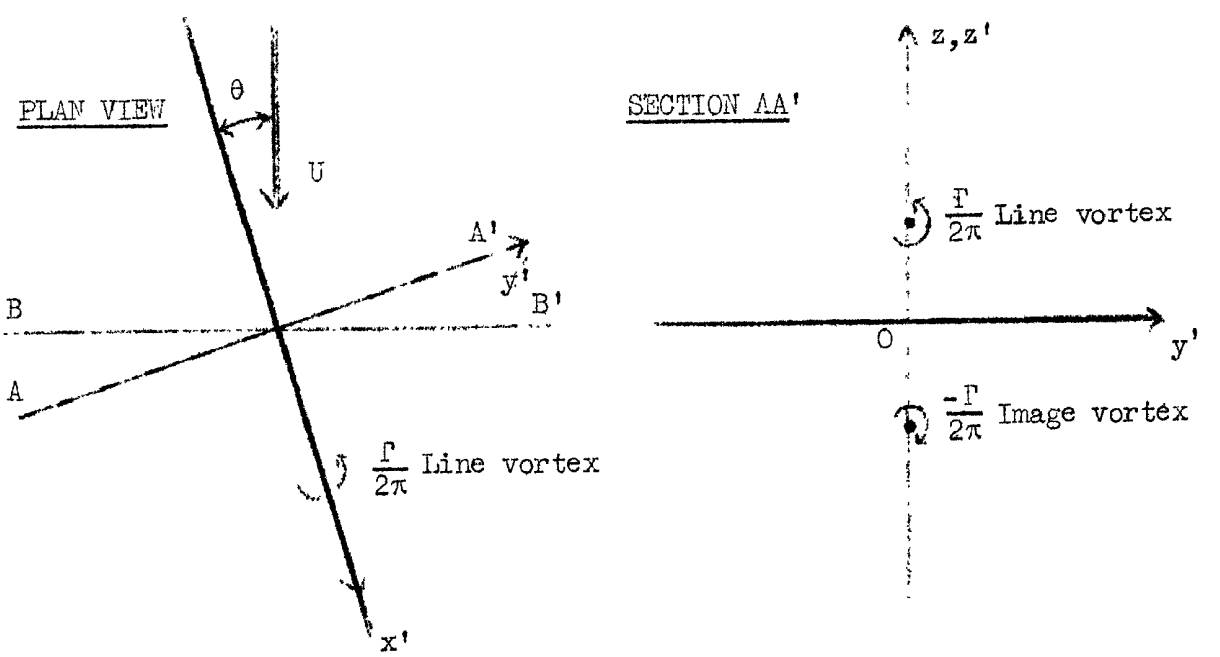

For the vortex to pass along a free streamline we have:-

$$\sin\theta = \frac{\Gamma}{2\pi U}\,\frac{1}{2Z_v} < 1 \qquad (37)$$

and the cross flow velocity v_v due to one vortex is:-

$$v_v = \frac{\Gamma}{2\pi}\,\frac{Z_v}{y^2 + Z_v^2} \qquad (38)$$

for points on the plane.

Now the pressure distribution with respect to the undisturbed stream pressure is:-

$$C_P = 1 - \left\{\cos^2\theta + \left(\frac{2\,v_v}{U} - \sin\theta\right)^2\right\} \tag{39}$$

$$= \frac{4\,v_v}{U^2}\,(U \sin\theta - v_v) \tag{40}$$

$$= \frac{\Gamma^2}{2\pi^2 U^2}\,\frac{y'^2 - Z_v^2}{(y'^2 + Z_v^2)^2} \tag{41}$$

along AA', and in terms of the co-ordinates of Fig.1 this becomes:-

$$C_P = \frac{\Gamma^2}{2\pi^2 U^2}\,\frac{\{(y - \Delta S_o')\cos\theta\}^2 - Z_v^2}{[\{(y - \Delta S_o')\cos\theta\}^2 + Z_v^2]^2} \tag{42}$$

$$= \frac{\Gamma^2}{2\pi^2 U^2}\,\frac{(A-D)^2\cos^2\theta - 1}{[(A-D)^2\cos^2\theta + 1]^2} \tag{43}$$

where $A = \frac{y}{Z_v}$, $D = \frac{\Delta S_o'}{Z_v}$.

We may determine the load coefficient per unit chord due to such a distribution

$$= \int_{BB'} C_P\,dy \tag{44}$$

and for infinite span

$$\int_{-\infty}^{\infty} C_p\,dy = \frac{\Gamma^2}{2\pi^2 U^2 \cos\theta}\int_{-\infty}^{\infty}\frac{\lambda^2 - 1}{(\lambda^2+1)^2}\,d\lambda = 0 \tag{45}$$

where $\lambda = (A-D)\cos\theta$.

Hence there is no contribution to the loading from such a system.

WT.2078.C.P.551.K3 - Printed in England

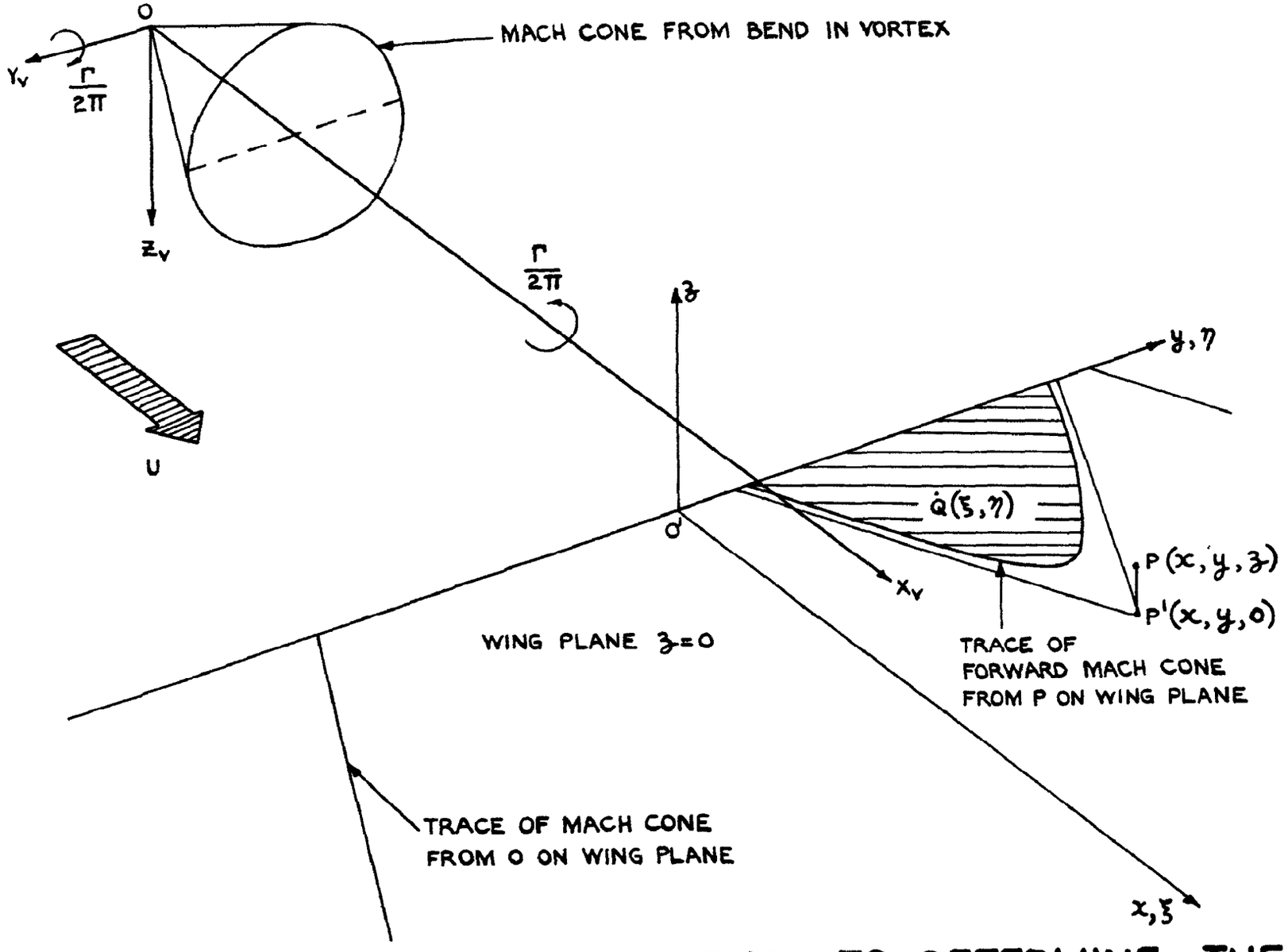

FIG. 1. AXES AND REGION OF INTEGRATION TO DETERMINE THE EFFECT OF THE WING AT P (x, y, z)

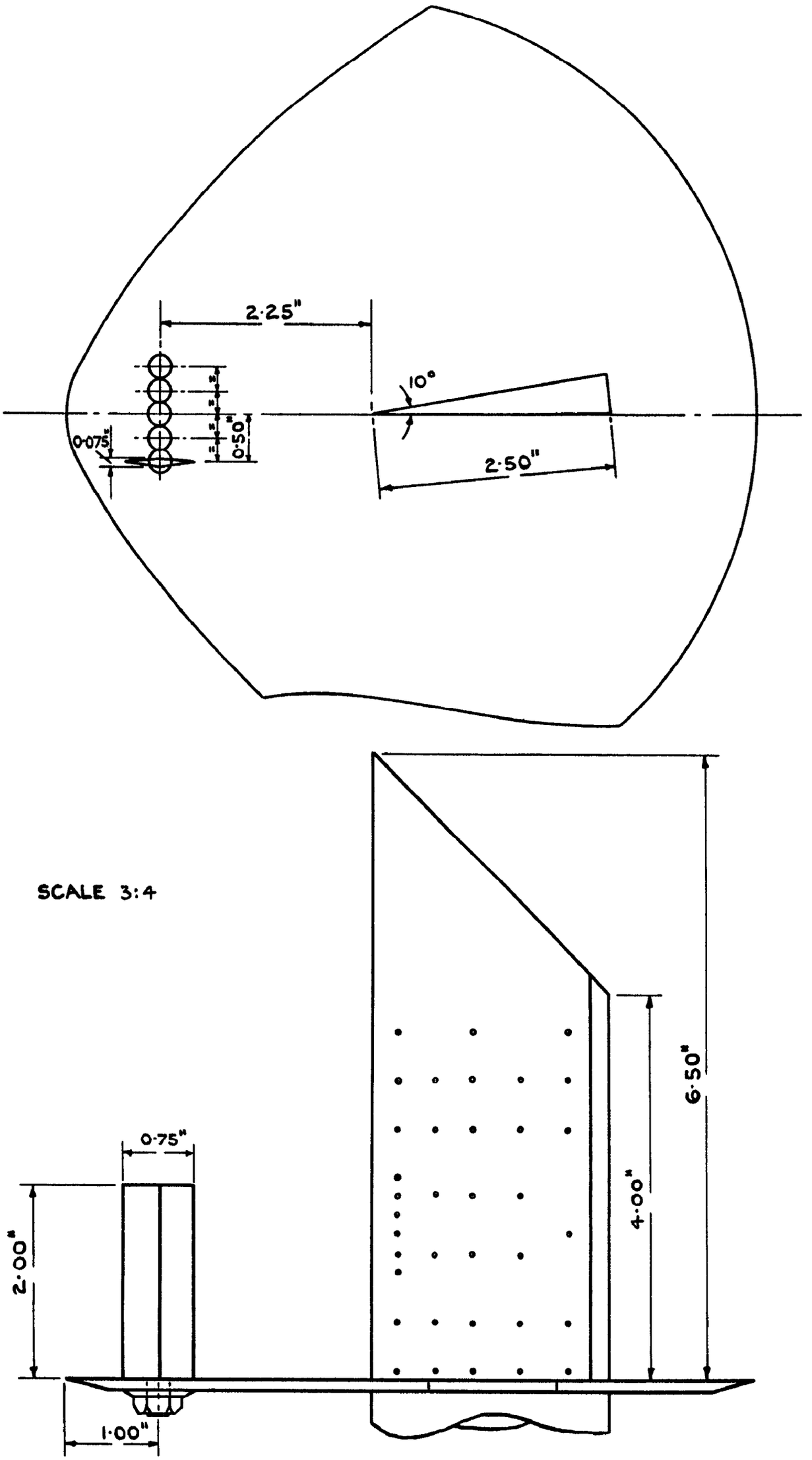

FIG. 2. DETAILS OF THE MODEL.

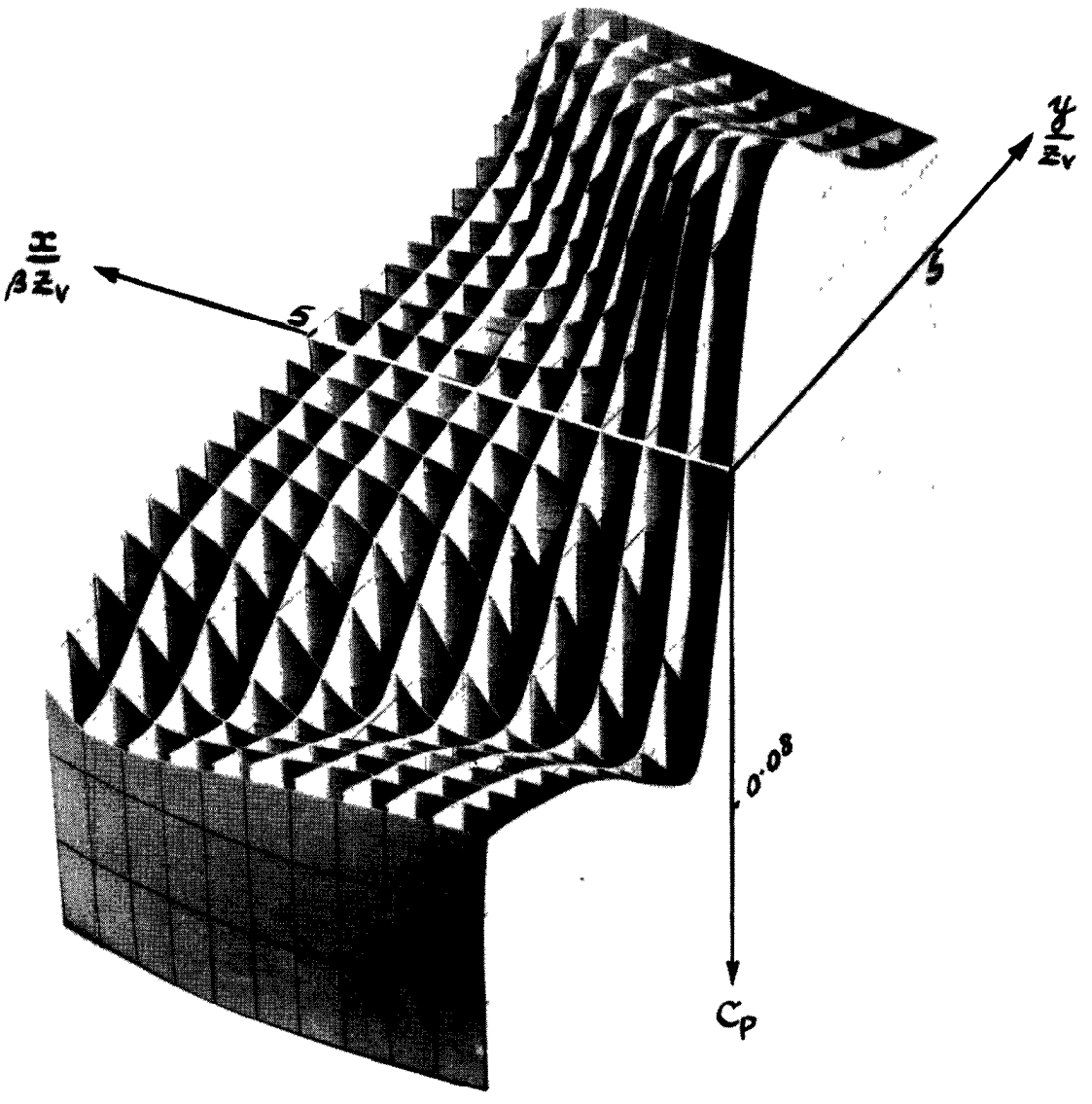

FIG.3. THEORETICAL SURFACE PRESSURE DISTRIBUTION DUE TO A VORTEX

$\frac{\Gamma}{u\, c_o} = 0.21$ (LINEARISED THEORY)

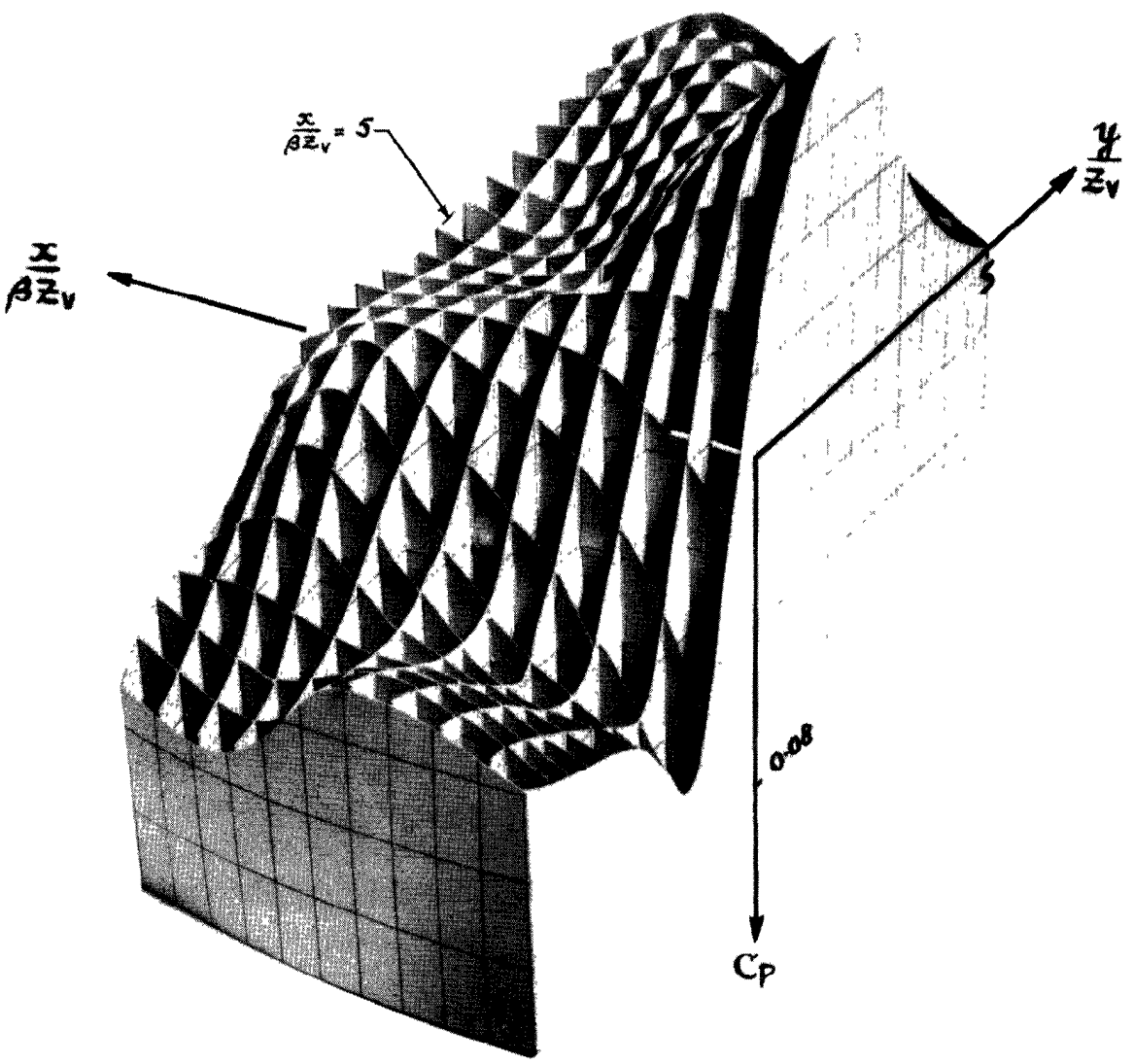

FIG.4. EXPERIMENTAL SURFACE PRESSURE DISTRIBUTION DUE TO A VORTEX

$\frac{\Gamma}{u c_o} = 0.21, \quad \delta = 10^o, \quad h = 0.25"$

(REFLECTION PLATE IS AT $\frac{y}{z_v} = -6.45$)

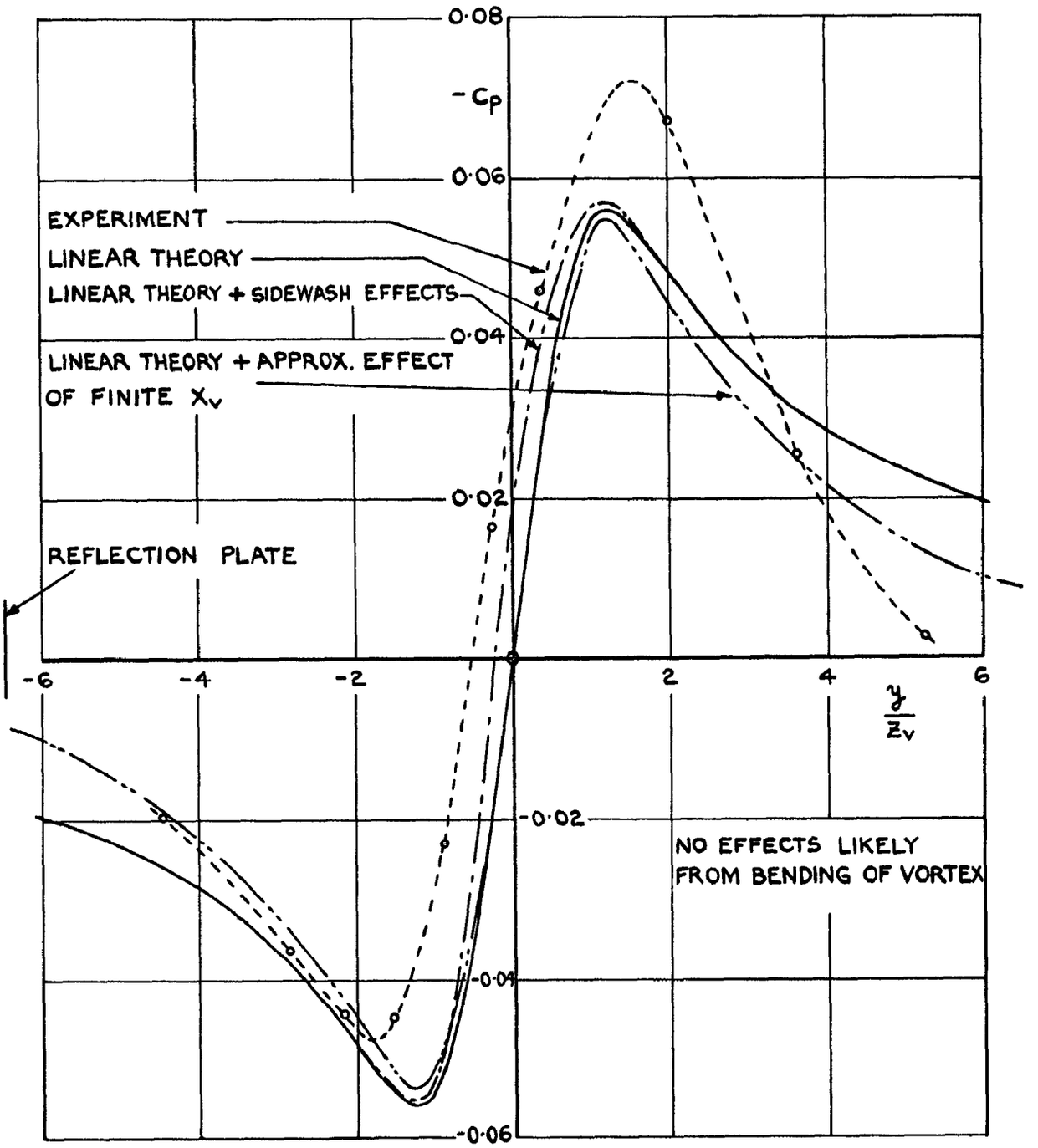

FIG.5. SURFACE PRESSURE DISTRIBUTION AT

$$\frac{x}{Z_v\beta} = 0{\cdot}60, \quad \frac{\Gamma}{Uc_0} = 0{\cdot}22, \quad \delta = 10^\circ, \quad h = 0{\cdot}25''.$$

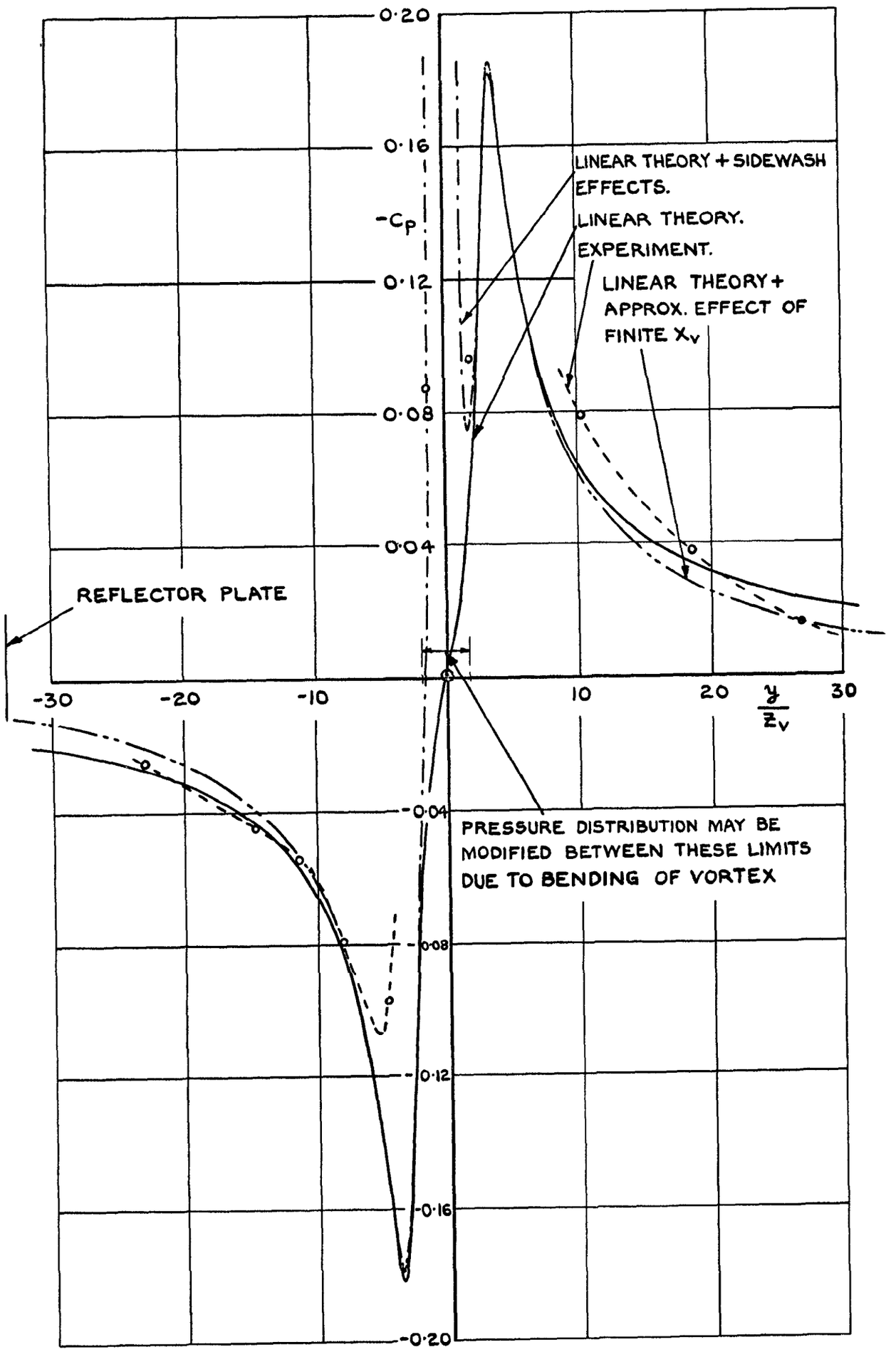

FIG.6. SURFACE PRESSURE DISTRIBUTION AT $\frac{x}{z_v\beta} = 3{\cdot}10$, $\frac{\Gamma}{Uc_0} = 0{\cdot}22$, $\delta = 10°$, $h = 0"$.

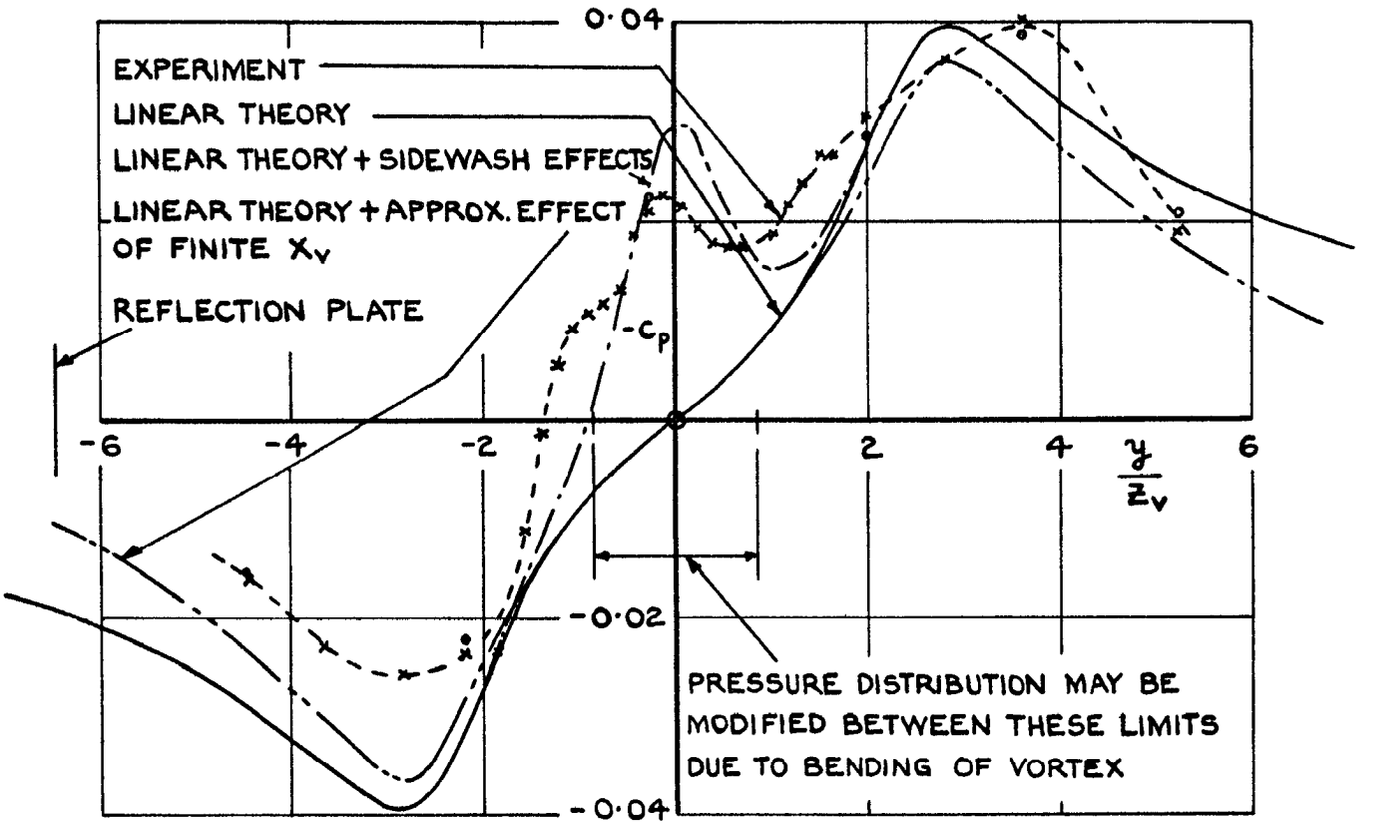

FIG. 7. SURFACE PRESSURE DISTRIBUTION AT $\frac{x}{z_v \beta} = 2{\cdot}30$, $\frac{\Gamma}{U c_0} = 0{\cdot}22$, $\delta = 10°$, $h = 0{\cdot}25''$.

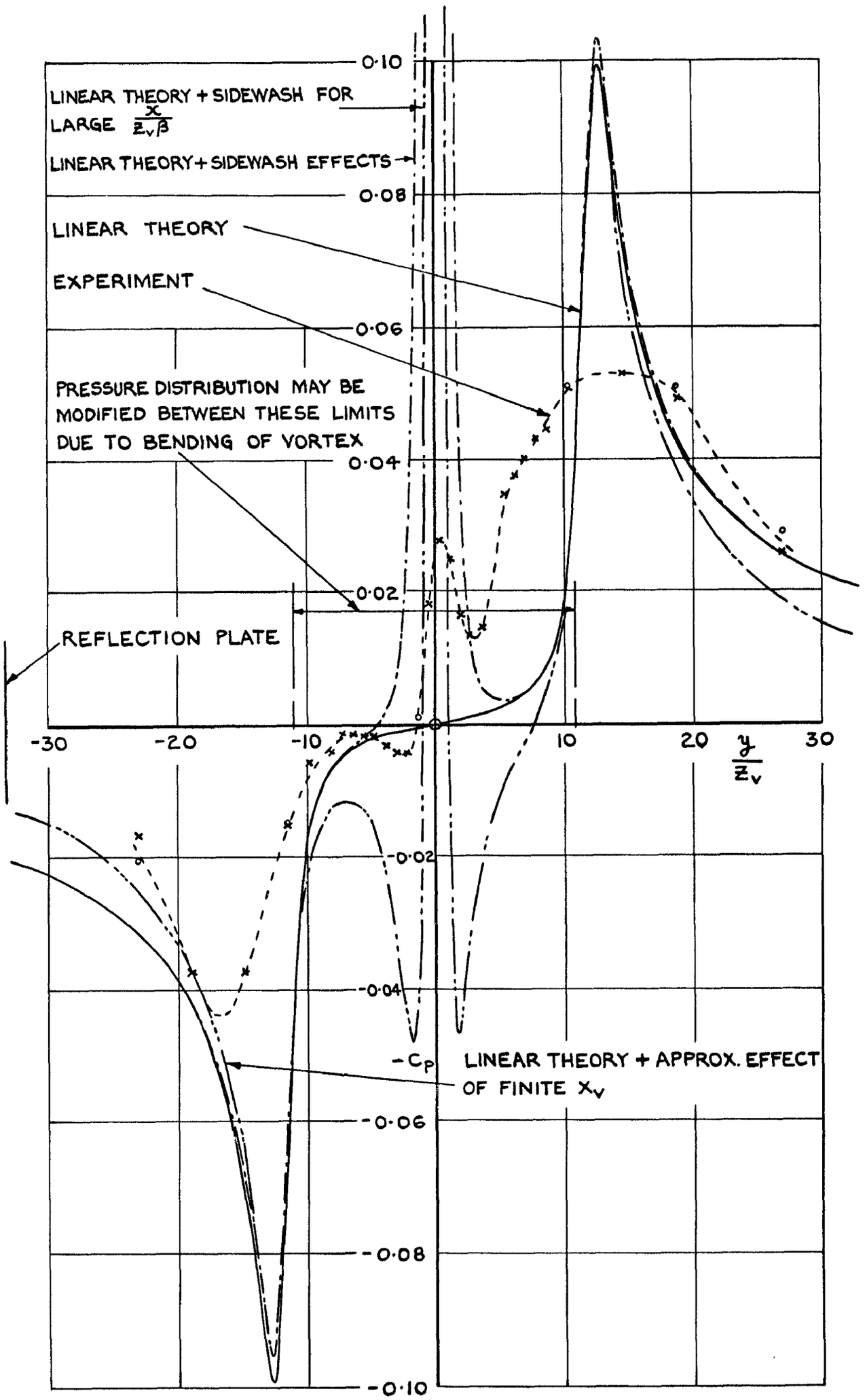

FIG.8. SURFACE PRESSURE DISTRIBUTION AT $\frac{x}{z_v\beta} = 12{\cdot}0$, $\frac{\Gamma}{Uc_0} = 0{\cdot}22$, $\delta = 10°$, $h = 0"$.

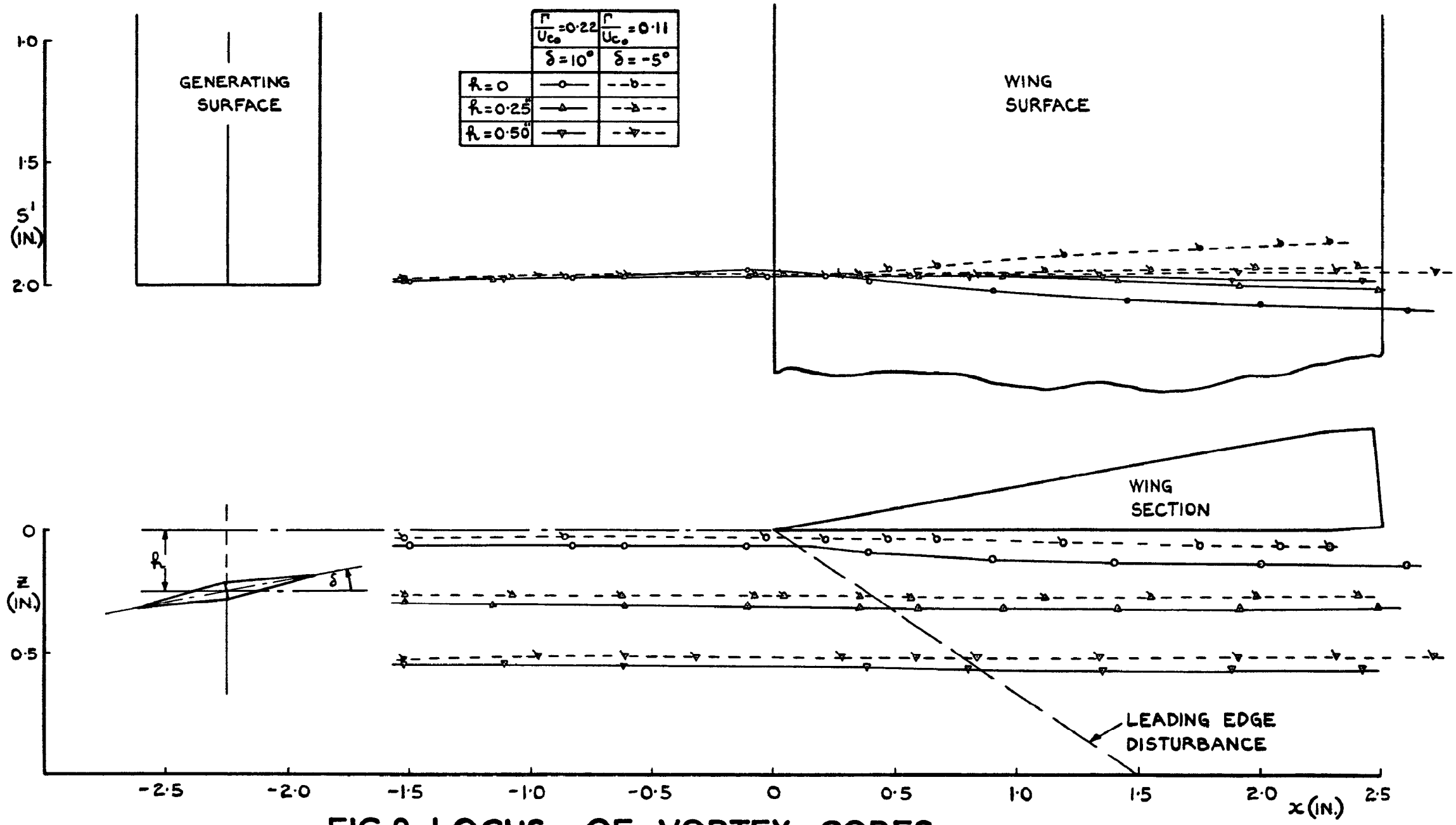

FIG. 9. LOCUS OF VORTEX CORES.

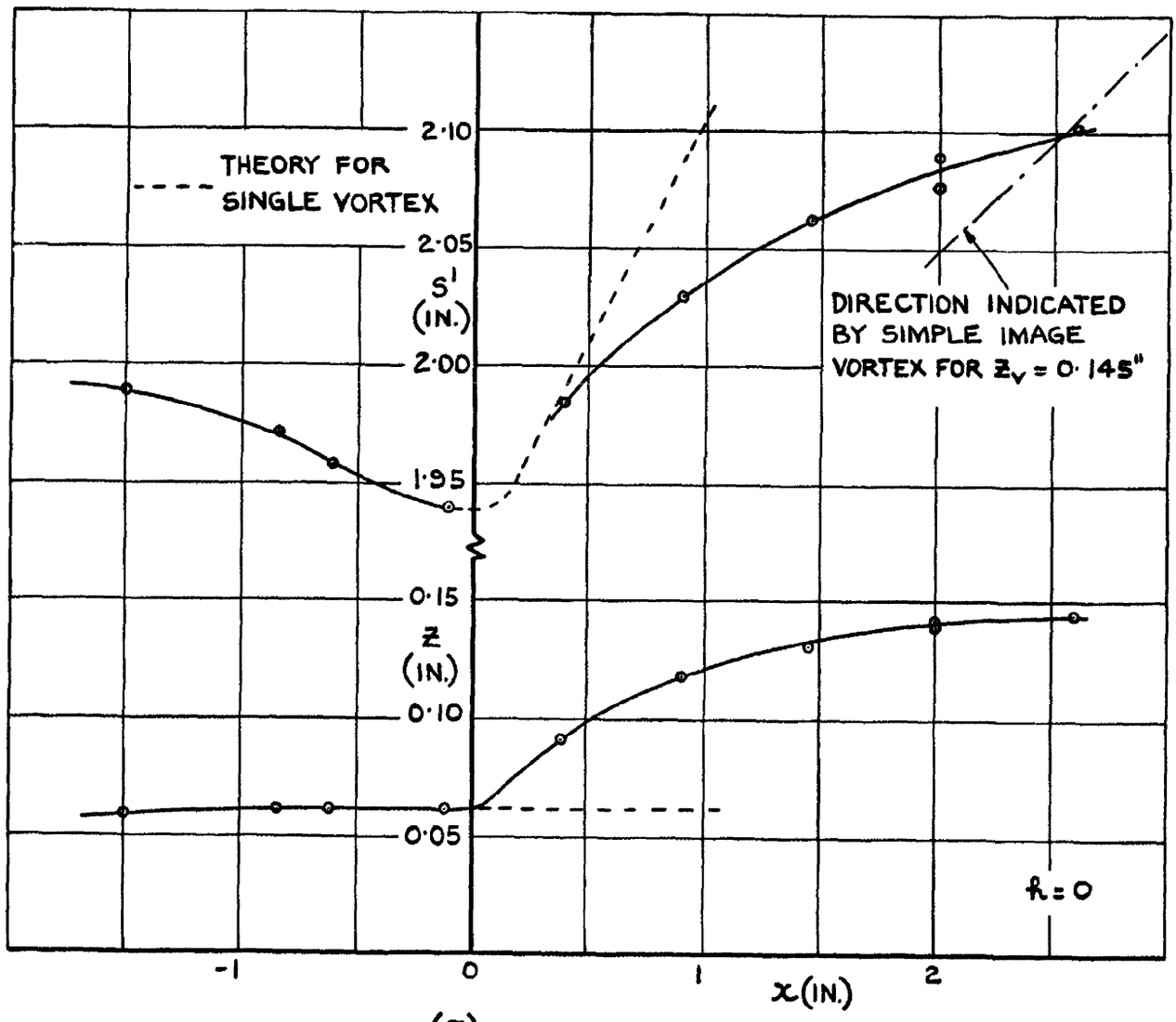

(a)

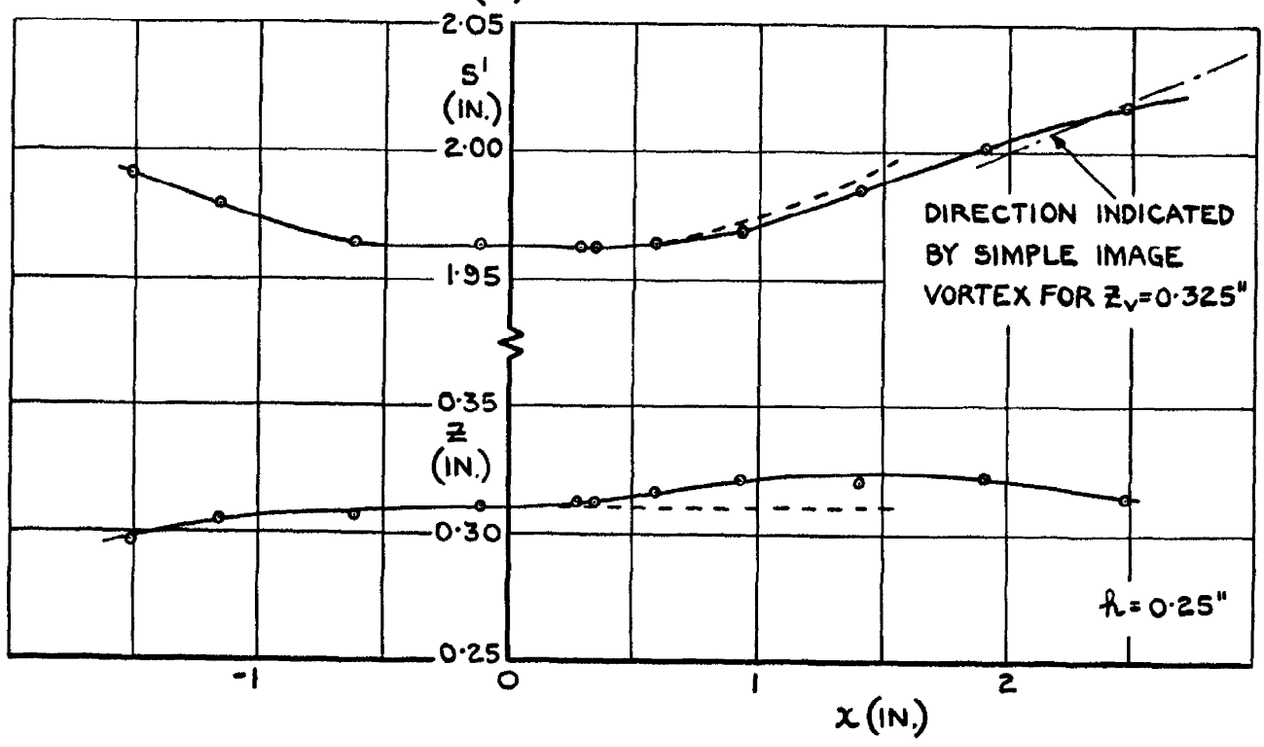

(b)

FIG. 10 (a&b). LOCUS OF VORTEX CORES
COMPARISON WITH THEORY $\frac{\Gamma}{U c_0} = 0{\cdot}22$, $\delta = 10°$.

A.R.C. C.P. No.551

533.69.048.2:
533.693:
533.6.011.5

A WIND TUNNEL INVESTIGATION INTO THE PRESSURE DISTRIBUTION ON A WING SURFACE IN A NON-UNIFORM SUPERSONIC FLOW.
Firmin, M.C.P. and Bartlett, W.J. Feb. 1960.

Using experimental and theoretical methods it is shown that linearized theory may be used to determine the pressure distribution on a wing surface in a non-uniform flow field caused by a streamwise line vortex.

It is demonstrated that a free vortex passing over a surface induces pressure and suction peaks on respective sides of the spanwise station of the vortex. These peaks are situated along Mach lines and are attenuated chordwise. It is found necessary to include the cross-flow terms in determining the theoretical pressure distribution.

A.R.C. C.P. No.551

533.69.048.2:
533.693:
533.6.011.5

A WIND TUNNEL INVESTIGATION INTO THE PRESSURE DISTRIBUTION ON A WING SURFACE IN A NON-UNIFORM SUPERSONIC FLOW.
Firmin, M.C.P. and Bartlett, W.J. Feb. 1960.

Using experimental and theoretical methods it is shown that linearized theory may be used to determine the pressure distribution on a wing surface in a non-uniform flow field caused by a streamwise line vortex.

It is demonstrated that a free vortex passing over a surface induces pressure and suction peaks on respective sides of the spanwise station of the vortex. These peaks are situated along Mach lines and are attenuated chordwise. It is found necessary to include the cross-flow terms in determining the theoretical pressure distribution.

A.R.C. C.P. No.551

533.69.048.2:
533.693:
533.6.011.5

A WIND TUNNEL INVESTIGATION INTO THE PRESSURE DISTRIBUTION ON A WING SURFACE IN A NON-UNIFORM SUPERSONIC FLOW.
Firmin, M.C.P. and Bartlett, W.J. Feb. 1960.

Using experimental and theoretical methods it is shown that linearized theory may be used to determine the pressure distribution on a wing surface in a non-uniform flow field caused by a streamwise line vortex.

It is demonstrated that a free vortex passing over a surface induces pressure and suction peaks on respective sides of the spanwise station of the vortex. These peaks are situated along Mach lines and are attenuated chordwise. It is found necessary to include the cross-flow terms in determining the theoretical pressure distribution.

Published by
HER MAJESTY'S STATIONERY OFFICE

To be purchased from
York House, Kingsway, London w.c.2
423 Oxford Street, London w.1
13A Castle Street, Edinburgh 2
109 St. Mary Street, Cardiff
39 King Street, Manchester 2
50 Fairfax Street, Bristol 1
2 Edmund Street, Birmingham 3
80 Chichester Street, Belfast 1
or through any bookseller

Printed in England

S.O. CODE No.23-9012-51